-RESEARCH PAPER

International Journal of Mining and Geo-Engineering

IJMGE

IJMGE 59-4 (2025) 341-348

DOI: 10.22059/IJMGE.2025.396195.595264

Rock mass integrity assessment using a site-specific discontinuity index: insights into fragmentation at the eureka delta gold mine

Kanongovere Makomborero Salachi [a, *], Raymond Sogna Suglo [a] and Munyindei Masialeti [a]

[a] *Botswana International University of Science and Technology, Palapye, Botswana.*

Article History:

Received: 28 May 2025.

Accepted: 27 August 2025.

ABSTRACT

This study introduces a Site-Specific Discontinuity Index (ssDI) to evaluate the influence of geological discontinuities on blast fragmentation efficiency at the Eureka Delta Gold Mine. The ssDI integrates eight structural parameters: volumetric joint count, joint orientation, persistence, infill condition, alteration, water content, and micro and macro-structural features. Validation was performed using Pearson correlation analysis, revealing a strong negative relationship between ssDI and fragmentation efficiency ($r = -0.77$) and a moderate positive relationship with Rock Mass Rating ($r = 0.56$). Additionally, fragmentation performance was evaluated across three ssDI categories (low, medium, high) using Welch's one-way ANOVA ($p = 2.26 \times 10^{-16}$), confirming significant differences between structural domains. To further validate the ssDI, particle size distributions (D_{50}, D_{80}, D_{99}) from WipFrag image analyses of 20 representative blasts were assessed across ssDI groups. The results showed that high ssDI zones produced finer but more variable fragmentation with larger oversize extremes, medium ssDI zones achieved the most uniform fragmentation and low ssDI zones yielded coarser but more consistent fragment sizes near the target specification. These findings confirm that the ssDI offers a robust, site-adaptive tool for optimising blast design and enhancing fragmentation predictability in structurally complex rock masses.

Keywords: *Site-Specific Discontinuity Index (ssDI), Rock Mass Rating (RMR), Blasting efficiency, Fragmentation, Pearson correlation, Wipfrag analysis.*

1. Introduction

The integrity of rock masses plays a critical role in determining the effectiveness of blasting operations in open pit mining. Geological discontinuities, such as joints, faults, and bedding planes disrupt the transmission of explosive energy, leading to unpredictable fragmentation outcomes that complicate material handling, crushing, and the overall operational efficiency [1, 2, 3, 4, 5, 6]. Structural parameters, including joint orientation, persistence, infill, and volumetric joint count, critically influence how blast energy is redirected and absorbed within the rock mass, thereby controlling fragmentation patterns [7, 8, 9, 10, 11, 12]. Specifically, joints parallel to the blast face often lead to the formation of large, blocky fragments, whereas steeper joint inclinations tend to produce finer fragmentation [13, 14, 15, 16].

Beyond macrostructural parameters such as joint spacing and aperture, microstructural features, including grain boundaries, mineralogical heterogeneity, and micro-joint networks, further modify the distribution of explosive energy during blasting [17, 18]. The presence of water within discontinuities and fractures also alters rock behaviour by cushioning explosive energy, reducing fracture propagation and increasing fragmentation variability [19, 20]. Similarly, chemically altered or infilled joints containing weaker materials such as clay or calcite absorb blast energy unevenly, leading to inconsistent breakage [21, 22]. As mining operations advance into increasingly complex geological terrains, accurate characterization and quantification of discontinuity parameters become essential for optimising blast design and improving mine productivity [23, 24, 25, 26, 27]. Although traditional rock mass classification systems such as the Rock Mass Rating (RMR), the Q-system, and the Geological Strength Index (GSI) have long provided standardized frameworks for assessing rock mass quality, several studies have highlighted their limitations for blasting applications [1, 2, 28]. In particular, these conventional systems often fail to adequately capture site-specific geological complexities, such as anisotropy, discontinuity variability, and localised structural conditions, which critically influence blast fragmentation outcomes [29, 30, 31]. These findings underscore the need for adaptable, detailed and site-specific predictive tools that extend beyond generalised rock mass descriptions.

Additional work has demonstrated that discontinuity spacing and general rock mass conditions significantly influence the median fragment size, using image analysis to develop empirical correlations [32]. However, their approach primarily focused on broad discontinuity parameters and did not fully integrate additional factors, such as infill material properties, degree of alteration, water content, and microstructural variability features which are increasingly recognised as essential for reliable fragmentation prediction. Building upon these recent advancements, the present study develops a Site-Specific Discontinuity Index (ssDI) to enhance the prediction of blast fragmentation behaviour in the structurally heterogeneous environment of the Eureka Delta Gold Mine. The ssDI integrates eight key structural parameters, such as volumetric joint count, joint orientation, persistence, infill condition, alteration, water content, and micro- and macrostructural features into a unified metric tailored to the local geological conditions. The objective of this study is to establish and

* Corresponding author. *E-mail address:* km23019027@biust.ac.bw (K. Makomborero Salichi).

validate the ssDI by correlating it with particle size distributions obtained through image analysis of post-blast muckpiles, thereby assessing its practical application for optimising fragmentation outcomes at the Eureka Delta Gold Mine.

1.1. Study site

The Eureka Delta Gold Mine is located within the Guruve District of Mashonaland Central Province, Zimbabwe, and forms part of the Guruve Greenstone Belt of the Zimbabwean Craton. The mine operates as an open pit excavation with multiple benches ranging from 1100 m to 1180 m elevation. Geologically, the site is characterised by granodiorite bedrock intruded by quartz and pegmatite veins, bounded by greenstone belts and crosscut by mafic dykes. Structurally, the rock mass exhibits steeply dipping joint sets with dip angles varying between 15° and 80°, closely spaced joints particularly in greenstone zones (average joint spacing less than 0.5 m) and persistent fault planes near lithological contacts. Hydrothermal alteration zones and groundwater seepage were also observed along major structural features, contributing to localised reductions in rock mass competence. Figure 1 illustrates the geological variations, presenting the layout of the excavation and the spatial distribution of significant lithological units. The geological complexity of the pit is further reflected by the transition between competent granodiorite zones and highly fractured, weathered greenstone in waste areas, necessitating site-specific considerations for blasting design and rock fragmentation prediction.

Figure 1: General layout of the Eureka Delta Gold Mine, showing pit boundaries and exposed lithological units.

2. Methods used

A structured field and data investigation programme was conducted at the Eureka Delta Gold Mine to characterise geological discontinuities, drilling conditions, and blast fragmentation performance. The dataset included (i) geological and geotechnical parameters gathered from field surveys and historical exploration records, (ii) production blasting records focusing on drilling and charging parameters, (iii) post-blast performance data, with a focus on fragmentation. A total of 110 production blasts were evaluated across benches ranging from 1100 m to 1180 m elevation which consisted of 20 newly observed blasts, supplemented by 90 pre-existing datasets.

2.1. Discontinuity parameter characterization

Structural discontinuities and their relative parameter data were collected through a structured approach combining field mapping, core logging, historical records, and geospatial modelling. The aim was to obtain robust and traceable discontinuity data necessary for developing the Site-Specific Discontinuity Index. Prior to field mapping, manual face mapping was conducted using a Brunton compass, digital clinometer, and tape measure, employing a 1 m × 1 m cell mapping technique. This facilitated the documentation of joint orientation (strike and dip), surface characteristics (e.g., planar, rough, weathered), persistence, aperture, infill type, and any indications of water seepage. Representative field photographs were taken during mapping, illustrating joint orientation, persistence, macrostructure, infill, and alteration, which directly contributed to the ssDI formulation, as shown in Figure 2.

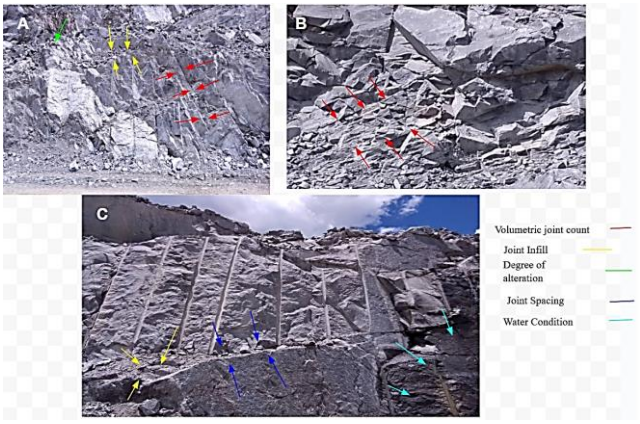

Figure 2: Discontinuities mapped at the Eureka Delta Gold Mine with (A) steeply dipping joints, (B) Close-up intersecting joints and (C) fault plane (inclined joint with uniform spacing).

In addition to primary field observations, secondary datasets, including window mapping records, drill core logs, and archived RMR values, were incorporated to supplement field structural data and support rock mass characterization. Drill core data offered a vertical perspective, highlighting joint continuity, Rock Quality Designation (RQD), alteration zones, and infill types at depth. Figure 3 displays a representative core tray from the Eureka Delta Gold Mine, showcasing key discontinuity features, such as intersecting fractures, varying joint persistence, and potential alteration zones. These visual observations were cross-referenced with logged data to improve the accuracy of the subsurface discontinuity parameters incorporated into the ssDI formulation. Moreover, a total of 270 geological data points were mapped and spatially linked to 110 production blast events.

Figure 3: Drill core tray from the Eureka Delta Gold Mine showing intersecting joints, variation in fracture persistence, and visible alteration zones.

2.2. Drilling blasting data collection

Drilling and blasting parameters were documented for each blast event to evaluate the interaction between geological structures and blasting outcomes. Waste benches (1100 - 1130 m) were drilled using 127 mm diameter bits with burden and spacing configurations of 3.1 m × 3.6 m, while ore benches (1150 - 1180 m) employed 115 mm diameter bits with 2.5 m × 2.8 m drill hole patterns. Powder factors ranged from 1.1 to 1.4 kg/m³, depending on the lithology and structural stability. Field observations recorded frequent borehole collapses and instances of drill

steel loss in structurally weak zones, particularly in benches affected by closely spaced joints, groundwater ingress, and fault planes, as illustrated in Figure 4. These instabilities compromised borehole integrity, disrupted drilling operations, and required frequent field adaptations, including sleeving and pre-stemming adjustments. These observations provided important operational context for analyzing the relationship between geological discontinuities and blast performance.

Figure 4: Field photographs showing (up) a collapsed blast hole due to poor ground conditions and (down) a lost drill steel rod embedded within fragmented muck at the Eureka Delta Gold Mine.

2.3. Fragmentation measurement

Post-blast fragmentation was assessed using a combination of field-based photographic capture and image analysis through WipFrag software. Immediately following each blast event, calibrated digital photographs of the muckpiles were systematically captured from three positions (crest, mid-slope, and toe) using a standardized procedure. Calibration scales of known dimensions were placed within each image frame to ensure consistency and accuracy during particle sizing analysis. Figure 5 illustrates the photographic and analytical workflow used to assess post-blast fragmentation. The muckpile image (Figure 5A) was captured with calibration scaling in place and processed using WipFrag for size distribution analysis. The software output (Figure 5B) displays fragmentation parameters essential for evaluating blast performance against the target threshold of 95% material passing a 450 mm sieve.

2.4. Formulation and validation of ssDI

To quantify the influence of structural discontinuities on blast fragmentation, a Site-Specific Discontinuity Index (ssDI) was developed for the Eureka Delta Gold Mine. The ssDI integrates eight geological parameters, each identified and characterized through detailed field investigations at the mine site. These parameters include: volumetric joint count (Jv), joint orientation (O), persistence (P), infill condition (I), degree of alteration (A), water presence (W), microstructural characteristics (Mi), and macrostructural features (Ma). The index is computed using the following expression:

$$ssDI = J_v \left[1 + \frac{1}{P} + \frac{2}{O} + \frac{1}{W} + \frac{0.5}{(M_i + M_a)} + \frac{1}{A} + \frac{1}{I}\right] \times k \quad (1)$$

Where: J_v = volumetric joint count; P = joint persistence; O = joint orientation; M_i = micro and M_a = macro structures; A = joint alteration; W = water content; I = joint infill.

The formulation of ssDI draws upon established rock mass classification methodologies, such as RMR, Q-system, and modified rock blockiness concepts, while adapting the weights and scoring ranges to reflect localised geological variability at the site [2, 33, 34]. All input parameters, except for joint orientation and joint volume, were standardized and categorized on a 10-point scale, informed by field observations, tactile assessments, and cross-validation with core logging data. In contrast, joint orientation and joint volume were incorporated using direct field measurements due to their quantitative nature and low interpretive variability. The volumetric joint count (Jv) served as the core multiplier, as joint density amplifies the combined effect of other discontinuity properties on fragmentation outcomes. A baseline constant (+1) is included in the ssDI to maintain index sensitivity under favourable conditions, consistent with additive components used in models like the Rock Mass Index [35]. Each factor in the ssDI formulation is inversely weighted according to its impact on rock mass stability, with the weighting scheme derived from established rock mass classification systems, such as the RMR system, GSI, and the Blastability Index [2, 28, 36]. Weighting coefficients were assigned based on both empirical observations at the Eureka Delta Gold Mine and supporting literature. The formula applies a weighted expression system as follows: 1/x for parameters with moderate influence (P, W, A, I), 2/x for joint orientation due to its significant effect on blast wave propagation, and 0.5/x for micro and macro structures to reflect their relatively secondary impact [37, 38]. A multiplicative scaling factor k was used to normalize the ssDI values, ensuring that the index is appropriately scaled for comparison across different bench levels and geological conditions at the mine site [2, 3, 25].

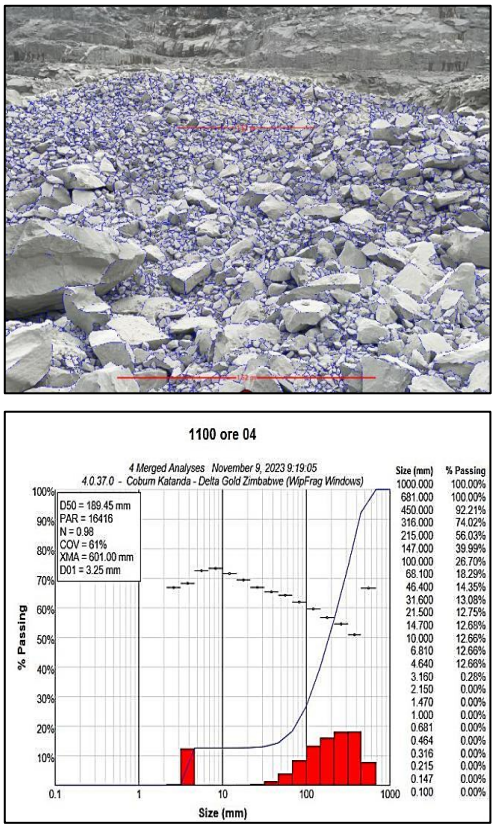

Figure 5: Post-blast muckpile image (up) and corresponding fragmentation analysis (down) using WipFrag software at the Eureka Delta Gold Mine.

2.5. Validation of ssDI

To validate the predictive capability and structural consistency of the Site-Specific Discontinuity Index, a two-stage statistical approach was adopted. The compiled dataset derived from geological, geotechnical and blasting records was first pre-processed using R programming software, utilizing the *dplyr* and *tidyr* packages for data cleaning, transformation, and structuring [39]. In the first stage of validation, a Pearson correlation test was applied to examine the relationship between ssDI values and a key fragmentation metric across 110 production blasts, following a statistical approach [40]. An additional correlation was conducted between ssDI and the RMR to assess the degree of conceptual alignment between the proposed index and established classification systems. This dual correlation analysis served to evaluate whether ssDI, despite being site-specific, maintained consistency with traditional rock mass frameworks while offering enhanced predictive value for fragmentation behaviour.

In the second stage of the analysis, ssDI values were grouped into three categories (low, medium, and high) to represent increasing degrees of structural complexity and joint intensity. These groupings were based on natural thresholds observed within the dataset to ensure operational clarity. To assess whether fragmentation outcomes differed significantly between the three ssDI zones, a Welch's one-way ANOVA was performed. This statistical method was selected for its robustness in handling datasets with unequal variances and sample sizes, a common feature in field-based geotechnical studies [41]. Additionally, 20 blasts spanning the different ssDI categories were randomly selected for detailed particle size distribution analysis. Fragmentation was quantified from WipFrag-generated image analysis curves, extracting three key percentile metrics. Fragmentation size distributions were assessed using three key percentiles which are D_{50}, D_{80} , and D_{99}. The D_{50} represents the median particle size, with 50% of material passing below 180 mm, D_{80} indicates the size below which 80% of the material passes (typically < 300 mm) and D_{99} defines the upper bound of fragmentation, representing 99% passing material, generally above 450 mm. These metrics provided a comprehensive assessment of the fragmentation behaviour associated with varying structural conditions. Together, the Pearson correlation test, Welch's one-way ANOVA analyses, and comparative analysis of fragmentation provide statistical validation for ssDI as a reliable predictor of fragmentation outcomes across structurally heterogeneous mining environments.

3. Results and discussion

This section presents the geological parameters influencing ssDI calculation, the variability and spatial distribution of ssDI in the pit areas of the mine, and the validation and analysis of ssDI in relation to fragmentation efficiency. This is followed by a discussion on the implications of these findings for blast design and mine optimisation.

3.1. Geological parameters influencing ssdi calculation

The ssDI integrates eight geological parameters extracted from detailed field mapping and geotechnical data at 270 locations across the Eureka Delta Gold Mine. These include volumetric joint count (Jv), joint orientation, persistence, infill condition, alteration, water content, and micro and macrostructural features. As shown in Table 1, Jv ranged widely (60 - 2000 joints/m³), reflecting zones of both massive and highly fractured rock. Joint orientation spanned from -71° to 277°, with subsets parallel to the blast face (e.g., 0° - 20°, 160° - 200°) and others steeply inclined (e.g., 60° - 90°). Infill ratings averaged 8.69, indicating high mineral content. These discontinuity properties critically influence how explosive energy is transmitted and dissipated during blasting [1, 8, 26].

3.2. Spatial Distribution and Variability of ssDI in Mine Pit Areas

The calculated ssDI values across 110 production blast locations ranged from 12.12 to 69.00, with a mean of 32.00 and a standard deviation of 12.12 (see Table 2). This spread reflects the heterogeneous structural conditions of the pit, particularly observed in the highly sheared greenstone lithological contacts. As illustrated in Figure 6, high ssDI values (indicated in orange/red) are predominantly concentrated near lithological transitions and fault zones. These regions are characterized by increased structural complexity, which disrupts the propagation of blast energy, leading to suboptimal fragmentation. In contrast, low ssDI zones (blue/green) correspond to more intact rock masses, which facilitate more efficient energy transfer and controlled fragmentation [42, 43, 44]. This spatial distribution highlights the importance of geological mapping in predicting blasting outcomes and optimizing energy application.

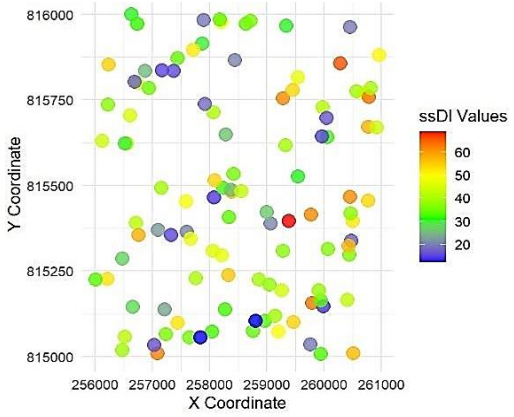

Figure 6: Distribution of ssDI at different geological points within mine pit areas.

3.3. Correlation of ssDI with fragmentation and RMR

To further understand the implications of ssDI variability, a regression and correlation test was performed to examine its relationship with fragmentation efficiency and Rock Mass Rating. As shown in Figure 7, there is a clear inverse relationship between ssDI and overall fragmentation efficiency, described by the regression equation *y = -1.36x + 155.79*. Moreover, the Pearson correlation test revealed a strong negative correlation (r = -0.77, see Figure 8), affirming the regression relationship which depicts that higher ssDI values associated with greater discontinuities and result in poorer fragmentation outcomes. In comparison, RMR values displayed a moderate, positive correlation with fragmentation (r = 0.56; see Figure 8). While high RMR values indicate better rock mass quality, the correlation is moderate, indicating the limitation of RMR. While RMR provides a general assessment of rock integrity, it does not capture localised discontinuities, which are critical to blast performance. Moreover, the observed correlations reinforce the predictive capability of ssDI over traditional measures like RMR. While RMR is effective for general rock mass assessments, ssDI provides more nuanced insights into energy dissipation paths, crucial for optimizing blast designs in structurally heterogeneous zones.

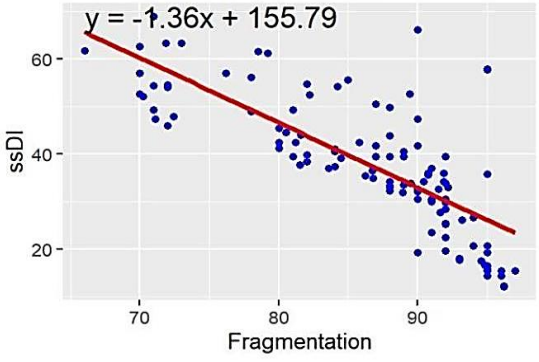

Figure 7: Scatter plot ssDI against fragmentation.

Table 1: Summary statistics for geological parameters used in ssDI calculation.

Parameter	Count	Mean	Std Dev.	Min	Lower quartile	Median	Upper quartile	Max
Joint Volume (Jv)	270	246.74	419.50	60	60	60	200	2000
Joint Orientation (O)	270	114.74	54.74	-71	82.25	100	142	277
Joint Persistence (Jp)	270	3.30	3.20	1	1	3	3	10
Joint Alteration (A)	270	1.49	0.55	1	1	1	2	3
Joint Infilling (I)	270	8.69	1.18	3	9	9	9	9
Water content (W)	270	1.58	0.94	1	1	1	2	5
Microstructures (Mi)	270	4.70	1.14	1	5	5	5	8
Macrostructures (Ma)	270	1.16	0.45	1	1	1	1	3

Table 2: Summary Statistics for ssDI.

Metric	Count	Mean	Std	Min	Lower quartile	Median	Upper quartile	Max
ssDI	110	12.96	12.12	12.12	32	37.4	49.4	69

This confirms that high concentrations of discontinuities dissipate energy along fracture planes, preventing effective rock breakage. Additionally, a moderate positive correlation (r = 0.56) was observed between ssDI and RMR, suggesting congruency between the two, as ssDI incorporates several parameters also present in the RMR system. This correlation shows that ssDI is an effective indicator of geological conditions, capturing essential features of rock mass integrity, reinforcing its validity as a reliable predictor for fragmentation. The results are consistent with the concept that discontinuities in rock masses disrupt energy transfer, thereby reducing blasting efficiency in fractured rock formations, as demonstrated in previous studies [8, 27].

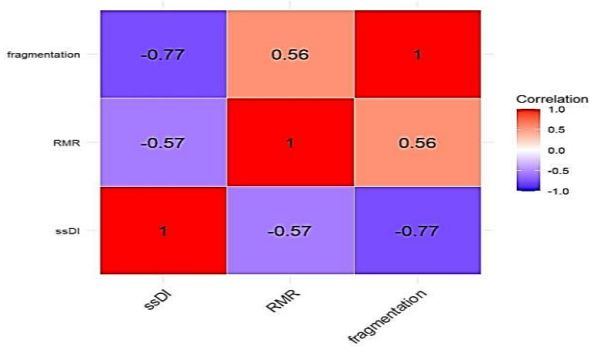

Figure 8: Pearson correlation matrix of ssDI, RMR and fragmentation.

3.4. Comparative fragmentation analysis across ssdi zones

To evaluate how fragmentation performance varies across different structural domains, ssDI values were grouped into three categories low (< 25), medium (25 - 45), and high (> 45). Figure 9 shows boxplots comparing overall fragmentation efficiency across the three groups. The results show a clear decreasing trend in fragmentation efficiency with increasing ssDI. Low ssDI zones achieved the highest and most consistent fragmentation outcomes, with fragmentation percentages clustering around 95%. Medium ssDI zones displayed slightly lower fragmentation values (88%), with moderate variability, while high ssDI zones showed the lowest fragmentation values (71%), along with the widest spread, indicating poor and inconsistent breakage performance. This trend indicates that as the complexity of a discontinuity increases, explosive energy is more likely to dissipate along fracture planes rather than contribute to efficient rock breakage. The broad spread of values in the high-ssDI category also suggests localised structural variation, which can produce unpredictable blast outcomes. Additionally, Welch's one-way ANOVA revealed a statistically significant difference in fragmentation across these three ssDI categories ($p = 2.26 \times 10^{-16}$), confirming that structural variability captured by the ssDI has a substantial effect on the degree of fragmentation.

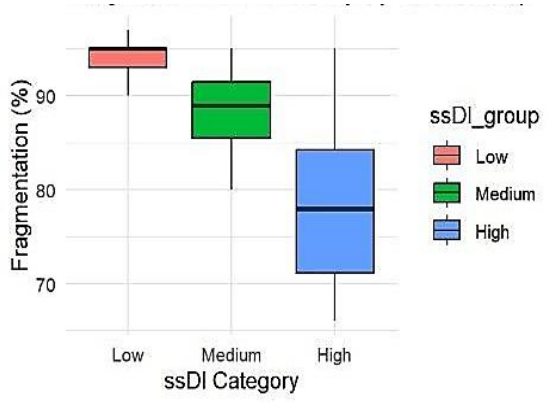

Figure 9: Box plots showing Fragmentation distribution in different ssDI zones.

Fragmentation size distribution analysis (D_{50}, D_{80}, D_{99})

To further validate the predictive capability of the ssDI, a subset of 20 production blasts was analysed for particle size distribution using WipFrag image analysis curves, as shown in Table 3. The selected blasts were drawn from across the pit and represented a broad spectrum of structural conditions, ranging from low to high ssDI values. For each blast, the fragmentation was quantified using three standard percentile metrics (D_{50}, D_{80} , and D_{99}).

Figure 10 presents boxplots comparing D_{50}, D_{80} , and D_{99} values across the three ssDI categories. The box plot analysis revealed clear differences in fragmentation behaviour across the ssDI zones. The plot shows that in high ssDI zones, characterised by dense and irregular fracture networks, fragmentation was generally finer but highly variable. Although the D_{50} values were lower, indicating a greater proportion of smaller fragments, D_{99} values often exceeded 600 mm, highlighting the presence of oversized fragments.

This variability arises from the irregular orientation and spacing of discontinuities, which can prematurely dissipate blast energy along weak planes [45, 32]. Similarly, it has been noted that in highly fractured rocks, energy disperses rapidly across existing joints, leading to localised zones of both excessive fines and coarse material [27]. This uneven energy distribution can leave certain large fragments intact, requiring secondary breakage, as observed by [26].

Table 3: Fragmentation Metrics by Blast ID and ssDI Zone.

Blast ID	D_{50}	D_{80}	D_{99}	ssDI	ssDI Category
Blast 1	178.6	323.0	460	12.5	Low
Blast 2	187.7	365.2	550	14.2	Low
Blast 3	250.3	540.2	700	25.3	Medium
Blast 4	135	230.4	350	30.5	Medium
Blast 5	92.7	312.9	320	32.1	Medium
Blast 6	150.6	300.6	600	45.6	High
Blast 7	160.4	405.5	500	40.0	High
Blast 8	110.3	250.2	400	35.7	Medium
Blast 9	120	190.9	380	22.0	Medium
Blast 10	175.4	310.4	700	20.3	Medium
Blast 11	135.2	265.1	480	48.5	High
Blast 12	148.6	270.5	500	15.3	Low
Blast 13	164	420	610	40.2	Medium
Blast 14	168.5	395.1	540	27.9	Medium
Blast 15	159.2	400.6	565	31.7	Medium
Blast 16	140.1	480	610	48.9	High
Blast 17	185.5	460.4	630	51.3	High
Blast 18	178.8	325.7	480	18.4	Low
Blast 19	190.3	360.9	530	22.1	Low
Blast 20	175.8	310.3	440	16.7	Low

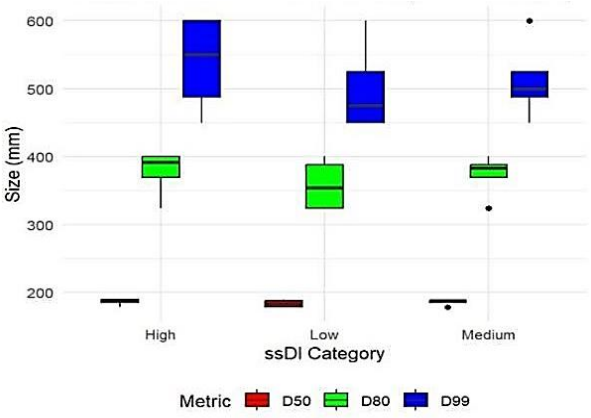

Figure 10: Boxplots comparing D50, D80, and D99 fragmentation metrics across low, medium and high ssDI.

Conversely, medium ssDI zones produced the most uniform fragmentation. D_{50} and D_{80} values clustered more tightly around the desired target size of 450 mm, with fewer extreme outliers in D_{99} values. This suggests that moderate joint densities promote optimal energy confinement: fractures are sufficient to assist breakage but not so dense as to excessively dissipate explosive energy [13]. Controlled energy release in these conditions results in more predictable and efficient fragmentation, enhancing downstream operations such as loading, hauling, and crushing. Furthermore, in low ssDI zones, where rock masses were relatively intact with fewer discontinuities, fragmentation outcomes were coarser but more consistent. D_{50} values ranged from 178 mm to 188 mm, while D_{99} values clustered around the target size, 450mm. The absence of abundant fracture planes means that explosive energy remains more concentrated, leading to larger but uniformly sized fragments. This observation is consistent with the finding that intact rock masses, although requiring more energy to break, produce fewer extreme fragmentation variances compared to heavily jointed rocks [8]. In brief, the strong inverse correlation between ssDI and fragmentation efficiency confirms that increasing discontinuity intensity and complexity negatively impact the quality of fragmentation. The observed trends across the three ssDI categories validate the use of ssDI as a predictive tool for blast performance, supporting previous findings on the critical role of geological structures in blast design optimisation.

3.5. Implications for blast design and mine optimization

The strong relationship between ssDI values and fragmentation outcomes highlights the critical importance of integrating structural geology into blast design strategies at the Eureka Delta Gold Mine. Tailoring blast parameters to the structural conditions identified through ssDI can significantly enhance energy confinement, improve the predictability of fragmentation and reduce operational inefficiencies. In high ssDI zones, where discontinuity density and structural complexity are greatest, blast designs should aim to mitigate premature energy dissipation. This can be achieved by reducing burden and spacing, optimising initiation sequences and moderating powder factors to minimise excessive fines. In medium ssDI zones, which exhibited the most favourable fragmentation characteristics, blast parameters should focus on maintaining energy balance, ensuring sufficient confinement without excessive fragmentation. Standard burden and spacing configurations with minor adjustments to powder factors are likely to yield optimal results. For low ssDI zones which are characterised by intact massive rock, higher powder factors and tighter drilling patterns may be necessary to concentrate explosive energy and achieve effective fragmentation. Designs should account for the presence of natural fracture planes by enhancing explosive energy delivery and minimising the risk of oversized fragments. The integration of ssDI analysis into pre-blast assessments offers a practical pathway for dynamic blast design adaptation, leading to improved fragmentation control, reduced secondary blasting, optimised equipment productivity and lower downstream processing costs.

4. Conclusions

The findings of this study underscore the pivotal role of incorporating the ssDI in optimising blast designs and enhancing fragmentation outcomes at the Eureka Delta Gold Mine. Unlike RMR, the ssDI enables a nuanced and localised evaluation of geological discontinuities,

equipping engineers with a precise tool to adapt blast strategies to the complex structural dynamics of the rock mass. This approach facilitates more efficient energy transfer, enhances fragmentation control, and significantly boosts operational efficiency. When integrated with RMR, ssDI forms a framework that addresses both the broad rock mass quality indicators and site-specific structural variations, thereby improving blast performance in geologically challenging environments. The results strongly show that ssDI should be adopted in the mine's rock mass assessment and blast design processes, offering a transformative means to fine-tune blasting operations and optimise overall mine productivity.

Acknowledgement

The authors gratefully acknowledge the Eureka Delta Gold Mine for granting access to the mine site and permitting field visits essential to this study. Special thanks are extended to KW Blasting and JRG for their invaluable assistance in data collection during the investigation.

References

[1] Bieniawski, Z.T., 1989. Engineering rock mass classifications: A complete manual for engineers and geologists in mining, civil, and petroleum engineering. Wiley, New York, pp. 45-67.

[2] Hoek, E. and Brown, E.T., 1997. Practical estimates of rock mass strength. *International Journal of Rock Mechanics and Mining Sciences*, 34(8), pp. 1165-1186.

[3] Hudson, J.A. and Harrison, J.P., 1997. *Engineering rock mechanics: An introduction to the principles*. Oxford: Pergamon, pp. 100-150.

[4] Hoek, E., Carranza-Torres, C. and Corkum, B., 2002. Hoek-Brown failure criterion – 2002 edition. *Proceedings of the NARMS-TAC Conference*, Toronto, 1, pp. 267-273. https://www.rocscience.com/documents/hoek/references/Hoek_2002.pdf.

[5] Rocchi, V., Tomio, P. and Pasquetto, A., 2014. Numerical modelling of blast-induced rock fragmentation in jointed rock masses. *International Journal of Rock Mechanics and Mining Sciences*, 67, pp. 32-41.

[6] Ghosh, A. and Daemen, J.J.K., 1983. A study of crack patterns in blasting. *International Journal of Rock Mechanics and Mining Sciences and Geomechanics Abstracts*, 20(1), pp. 39-47.

[7] Brady, B.H.G. and Brown, E.T., 2006. *Rock mechanics: For underground mining*. 3rd ed. London: Springer, pp. 101-120.

[8] Elmo, D. and Stead, D., 2015. An integrated numerical modelling - discrete fracture network approach applied to the characterisation of joint persistence. *Rock Mechanics and Rock Engineering*, 48(1), pp. 225-244.

[9] Singh, R., Maheshwari, B.K. and Gokhale, S., 2016. Influence of infill material on blast performance and fragmentation. *Journal of Mining Science*, 52(2), pp. 245-256.

[10] Wang, X., Li, X. and Yang, Z., 2018. Effects of joint orientation and dip on blast-induced damage in rock masses. *Engineering Geology*, 244, pp. 98-106.

[11] Cao, R., Li, X. and Huang, F., 2020. Influence of joint persistence on rock fragmentation using the finite-discrete element method. *Computers and Geotechnics*, 118, p.103304.

[12] Khandelwal, M. and Singh, T.N., 2009. Prediction of blast-induced ground vibration using artificial neural network. *International Journal of Rock Mechanics and Mining Sciences*, 46(7), pp. 1214-1222.

[13] Tulu, I.B. and Heasley, K.A., 2017. The role of joint orientation on pillar stability in underground mining. *International Journal of Rock Mechanics and Mining Sciences*, 93, pp. 69-79.

[14] Abass, H.H. and Misra, A., 2018. Effect of joint orientation on rock fragmentation and strength under different stress regimes. *Journal of Rock Mechanics and Geotechnical Engineering*, 10(2), pp. 231-240.

[15] Liu, D. and He, Z., 2019. Effect of microstructure on rock fragmentation and energy dissipation. *Geomechanics and Geophysics for Geo-Energy and Geo-Resources*, 5(3), pp. 297-309.

[16] Saroglou, H. and Tsiambaos, G., 2018. The influence of rock macro- and microstructure on uniaxial compressive strength: A comprehensive review. *Engineering Geology*, 245, pp. 130-144.

[17] Jing, H., Zhang, G., Zhang, X. and Duan, K., 2020. Effect of micro- and macro-scale structural features on rock fragmentation in mining. *Engineering Geology*, 271, p. 105612.

[18] Yang, S.Q. and Zhang, Y.C., 2019. Experimental investigation on the mechanical behaviour of sandstone with different water contents under uniaxial compression. *Geomechanics and Geophysics for Geo-Energy and Geo-Resources*, 5(3), pp. 297-309.

[19] Liu, D., Liu, Z. and Chen, Z., 2021. Water saturation effects on rock damage and energy dissipation in mining-induced dynamic loading. *Journal of Rock Mechanics and Geotechnical Engineering*, 13(3), pp. 662-673.

[20] Karakul, H. and Ulusay, R., 2017. Effect of joint infillings on the mechanical properties of rock discontinuities: An experimental approach. *Rock Mechanics and Rock Engineering*, 50(10), pp. 2621-2639.

[21] Kumar, R., Singh, P.K. and Singh, R., 2021. Impact of joint alteration and infill material on rock mass strength and stability during blasting. *Journal of Geotechnical and Geoenvironmental Engineering*, 147(9), p. 04021121.

[22] Jimeno, C.L., Jimeno, E.L. and Carcedo, F.J.A., 1995. *Drilling and blasting of rocks*. Rotterdam: Balkema, pp. 120-135.

[23] Hustrulid, W., 1999. *Blasting principles for open pit mining*. Boca Raton: CRC Press, pp. 145-153.

[24] Palmström, A., 2014. Measurements of and correlations between block size and rock quality designation (RQD). *Tunnelling and Underground Space Technology*, 40, pp. 60-73.

[25] Zhang, L., Zhang, L. and Chen, H., 2016. Estimation of volumetric joint count from joint traces on borehole walls. *International Journal of Rock Mechanics and Mining Sciences*, 83, pp. 243-253.

[26] Zhang, L., Zhang, L. and Chen, H., 2019. Influence of joint orientation on fragmentation patterns. *Journal of Mining Science*, 56(3), pp. 100-110.

[27] Hoek, E., Marinos, P. and Tsiambaos, G., 1995. The Geological Strength Index (GSI): A new tool for the classification of rock masses. *Tunnelling and Underground Space Technology*, 10(2), pp. 193-211.

[28] Singh, R. and Roy, A., 2020. A comparative study on site-specific modifications to conventional rock mass classification systems. *Journal of Rock Mechanics and Geotechnical Engineering*, 23(3), pp. 175-185.

[29] Zhao, X., Liu, Y., and Zhang, L., 2021. Modelling of blasting-induced fractures in jointed rock masses: A case study. *International Journal of Rock Mechanics and Mining Sciences*, 142, pp. 105080.

[30] Li, Q., Li, Y., and Wu, X., 2022. Effect of rock mass anisotropy on blast-induced rock fragmentation. *Geotechnical Testing Journal*, 45(5), pp. 123-135.

[31] Azizi, A. and Moomivand, H., 2021. A new approach to represent impact of discontinuity spacing and rock mass description on

the median fragment size of blasted rocks using image analysis of rock mass. *Rock Mechanics and Rock Engineering*, 54, pp. 2013-2038.

[32] Palmström, A., 2005. The Rock Mass Index (RMi) and its application to rock blasting operations. *Journal of Geotechnical Engineering*, 57(2), pp. 55-65.

[33] Lyana, N., Thomas, P., and McCrory, A., 2016. Joint orientation and blast wave propagation in fragmented rock. *Geotechnical Engineering Review*, 12(1), pp. 30-45.

[34] Choudhary, A. and Agrawal, R., 2022. Micro and macrostructural features affecting rock fragmentation. *Engineering Geology*, 245, pp. 50-70.

[35] Lilly, M., 1986. The application of blastability indices in rock mass classification. *International Journal of Rock Mechanics and Mining Sciences*, 26(1), pp. 11-19.

[36] Hoek, E. and Brown, E.T., 1980. Empirical strength criterion for rock masses. *Journal of Geotechnical Engineering*, 106(2), pp. 361-382.

[37] Bieniawski, Z.T., 1989. The development of the Rock Mass Rating (RMR) system. *Journal of Geotechnical Engineering*, 5(6), pp. 14-25.

[38] R Core Team, 2023. *R: A language and environment for statistical computing*, R Foundation for Statistical Computing, Vienna, Austria. https://www.r-project.org/.

[39] Soufi, A., Bahi, L., Oouadif, L. and Kissai, J.E., 2018. Correlation of rock mass classification parameters obtained from bore core and in situ observations. *MATEC Web of Conferences*, 149, 02030.

[40] Czinder, B. and Török, Á., 2021. Strength and abrasive properties of andesite: relationships between strength parameters measured on cylindrical test specimens and micro-Deval values. *Bulletin of Engineering Geology and the Environment*, 80, pp. 8871-8889.

[41] Mohanty, P., 1990. Blast-induced structural damage in rock masses. *Geomechanics and Geoengineering*, 10(4), pp. 47-56.

[42] Bhandari, K., 1997. Understanding energy dissipation in fractured rocks. *Journal of Mining Science*, 33(1), pp. 97-103.

[43] Khaoula, S., 2023. Understanding the role of discontinuity in blast fragmentation. *Journal of Geotechnical Engineering*, 12(2), pp. 102-118.

[44] Mwale, T., 2015. Phenomenology of control blasting in close proximity to densely populated communities - A case study of Mopan's area J open pit, Doctoral dissertation, The University of Zambia, pp. 20-49.